

An improved multi-exposure approach for high quality holographic femtosecond laser patterning

Chenchu Zhang, Yanlei Hu, Jiawen Li, Zhaoxin Lao, Jincheng Ni, Jiaru Chu, Wenhao Huang, and Dong Wu

Citation: *Appl. Phys. Lett.* **105**, 221104 (2014); doi: 10.1063/1.4902925

View online: <https://doi.org/10.1063/1.4902925>

View Table of Contents: <http://aip.scitation.org/toc/apl/105/22>

Published by the [American Institute of Physics](#)

Articles you may be interested in

[Two-photon polymerization of cylinder microstructures by femtosecond Bessel beams](#)

Applied Physics Letters **105**, 041110 (2014); 10.1063/1.4891841

[Direct laser writing of complex microtubes using femtosecond vortex beams](#)

Applied Physics Letters **110**, 221103 (2017); 10.1063/1.4984744

[Highly uniform parallel microfabrication using a large numerical aperture system](#)

Applied Physics Letters **109**, 021109 (2016); 10.1063/1.4955477

[Two-photon polymerization of a three dimensional structure using beams with orbital angular momentum](#)

Applied Physics Letters **105**, 061101 (2014); 10.1063/1.4893007

[High-efficiency fabrication of aspheric microlens arrays by holographic femtosecond laser-induced photopolymerization](#)

Applied Physics Letters **103**, 141112 (2013); 10.1063/1.4824307

[Femtosecond laser three-dimensional micro- and nanofabrication](#)

Applied Physics Reviews **1**, 041303 (2014); 10.1063/1.4904320



Lake Shore
CRYOTRONICS

Measure Ready
155 Precision I/V Source

A new current & voltage source
optimized for scientific research

LEARN MORE ▶

The image shows a Lake Shore Measure Ready 155 Precision I/V Source. The device is a rectangular, silver-colored unit with a black front panel. On the left side, there is a color LCD screen displaying 'AC Peak Amplitude 10.0000 mV', 'Frequency 100.000 kHz', and 'DC Offset 0.0000 mV'. To the right of the screen are several control buttons and a rotary switch. On the right side of the device, there are two sets of terminals: one for current (red and black) and one for voltage (red and black). The Lake Shore logo and 'Measure Ready 155 Precision I/V Source' are printed on the right side of the front panel.

An improved multi-exposure approach for high quality holographic femtosecond laser patterning

Chenchu Zhang, Yanlei Hu,^{a)} Jiawen Li,^{a)} Zhaoxin Lao, Jincheng Ni, Jiaru Chu, Wenhao Huang, and Dong Wu

Department of Precision Machinery and Precision Instrumentation, University of Science and Technology of China, Hefei 230026, China

(Received 20 October 2014; accepted 16 November 2014; published online 1 December 2014)

High efficiency two photon polymerization through single exposure via spatial light modulator (SLM) has been used to decrease the fabrication time and rapidly realize various micro/nanostructures, but the surface quality remains a big problem due to the speckle noise of optical intensity distribution at the defocused plane. Here, a multi-exposure approach which used tens of computer generate holograms successively loaded on SLM is presented to significantly improve the optical uniformity without losing efficiency. By applying multi-exposure, we found that the uniformity at the defocused plane was increased from ~ 0.02 to ~ 0.6 according to our simulation. The fabricated two series of letters “HELLO” and “USTC” under single-and multi-exposure in our experiment also verified that the surface quality was greatly improved. Moreover, by this method, several kinds of beam splitters with high quality, e.g., 2×2 , 5×5 Daman, and complex nonseparate 5×5 , gratings were fabricated with both of high quality and short time (< 1 min, 95% time-saving). This multi-exposure SLM-two-photon polymerization method showed the promising prospect in rapidly fabricating and integrating various binary optical devices and their systems.

© 2014 AIP Publishing LLC. [<http://dx.doi.org/10.1063/1.4902925>]

Femtosecond laser two-photon polymerization (TPP) microfabrication with both of high efficiency and high quality has attracted great attention because it can significantly decrease the fabrication time and cost^{1,2} of conventional TPP, which was based on single-beam point-to-point scanning.^{3,4} A variety of methods such as introducing microlens arrays (MLAs),⁵ spatial light modulator (SLM),⁶ or diffractive beam splitter⁷ to split incident light into several beams have been developed for high efficiency TPP. Among these methods, one of the most widely used ones is SLM due to its high flexibility of parallel fabrication. The distributions of foci array can be arbitrarily controlled by designing the computer generate hologram (CGH) on SLM.⁸ With this approach, a variety of optical,⁹ mechanical,¹⁰ and biological¹¹ microstructures have been rapidly fabricated. However, this method is only suitable for fabricating microstructure arrays with the same morphology by multi foci scanning.^{11,12} Moreover, this method is still based on the point-to-point scanning strategy, and thus cost long time to fabricate a 3D microstructure with bigger size, e.g., > 50 – $100 \mu\text{m}$.

In recent years, single-exposure fabrication of a certain structure via fs laser beam shaping has been proposed because of its high flexibility to fabricate non-array structures. Bessel beam, vortex beam and other shaped beams have been also used for fabricating some specific microstructures, e.g., microtubes.^{13–15} But the shapes of these beams are limited and could not be freely controlled,¹⁶ which seriously restricts the practical applications of these methods. A single-shot mode using digital mirror device (DMD) to load CGHs containing information of patterns has been used for

fabricating various structures via single exposure.¹⁷ But, the power efficiency of DMD is low to $\sim 20\%$ for generating complex patterns as it only modifies the amplitude of the incident light.

A phase-modulated SLM such as liquid crystal on silicon (LCoS) loads the phase information of desired pattern, and thus can get higher efficiency to $\sim 40\%$. But a continuous light field at focal plane has serious speckle noise,¹⁸ which ultimately results in low-quality flawed structures.¹⁹ In this letter, a multi-exposure technique using tens of CGHs successively loaded on SLM has been developed to eliminate speckle noise and fabricate microstructures with high quality through TPP. First, our simulation showed that the speckle noise and flawed structures were caused by the nonuniformity of optical field distribution at the defocused plane. We found that the uniformity increased from ~ 0.02 to ~ 0.6 by applying multi-exposure. Then, two series of letters were fabricated through a single exposure and multi exposure for comparison, which demonstrated that the multi-exposure approach can greatly improve the surface quality without any lose in efficiency. Finally, several kinds of complex beam splitters with high quality were rapidly fabricated, which further showed its high flexibility in realizing various binary optical devices.

Figure 1(a) shows a schematic diagram of experimental setup for femtosecond laser direct-writing. The laser source is a mode-locked Ti:sapphire ultrafast oscillator (Coherent, Chamleon Vision-S) with central wavelength at 800 nm, pulse duration of 75 fs, and repetition rate at 80 MHz. After passing a beam collimation system and a 4f configuration, femtosecond laser pulses are tightly focused into one Gaussian spot by the objective lens to induce TPP. Figure 1(b) is a diagram of single exposure mode using LCoS which

^{a)} Author to whom correspondence should be addressed. Electronic addresses: huyl@ustc.edu.cn and jwl@ustc.edu.cn

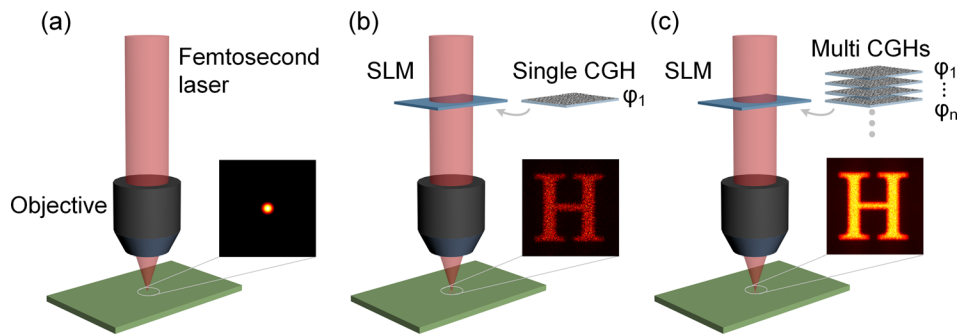


FIG. 1. (a) Schematic diagram of femtosecond laser direct laser writing. The optical intensity distribution at the focal plane is a round point. (b) Schematic diagram of single-exposure holographic femtosecond laser direct patterning. The optical intensity distribution at the defocused plane is a complex pattern “H” designed by CGH. However, the distribution shows low signal-to-noise and leads to low surface quality in fabricating micro/nanostructures. (c) Multi-exposure holographic femtosecond laser direct patterning. The optical intensity distribution at the defocused plane is a complex pattern “H” designed by multi-CGH with different phase. Due to the improved strategy, the distribution shows high signal-to-noise and thus high quality micro/nanostructures will be realized.

can significantly enhance the efficiency of single beam scanning [Fig. 1(a)]. Before being focused by the objective lens, the laser beam irradiates onto a reflective liquid crystal on silicon (Holoeye, Pluto NIR-2, resolution of 1920×1080 , pixel pitch of $8 \mu\text{m}$, and diagonal of 0.7 in.). So, designable computer-generated holograms are encoded on the central 1080×1080 pixels to generate various desired patterns. A $100\times$ microscope objective lens is used to focus the phase-modulated femtosecond laser beam into the sample. The optical field distribution in the sample is disjointed which will introduce flawed structures. Figure 1(c) is a diagram of multi-exposure using LCoS. The experiment setup is the same as that in Fig. 1(b) except that multi-CGHs containing the multi-phase information of a same pattern were successively loaded on SLM comparing to only 1 CGH in Fig. 1(b). The multi-CGHs are calculated by weighted Gerchberg-Saxton (GSW) algorithm²⁰ with different initial phases, which lead to different distribution of speckle noise. By this way, the noises can be averaged by multi-CGHs and the optical uniformity can be significantly improved, thus better microstructures were produced than those achieved by the approach in Fig. 1(b).

To deeply investigate the formation reason of flawed and discontinued structures, we simulate the optical intensity

distribution at the focal plane of objective lens. The CGHs are calculated by GSW to ensure the uniformity of focused pattern. Figure 2(a) is the simulation of intensity distribution at the focal plane of objective lens. Its uniformity of the letter “E” can reach as much as 0.98 by applying the GSW. However, when there is a small shift of 856 nm along z axis to the focal plane, the uniformity of intensity distribution has greatly seriously decreased to only 0.1, as shown in Fig. 2(b). As the depth of polymeric area is bigger than $1 \mu\text{m}$, the deterioration of optical uniformity at the defocused plane will result in flawed structures. So, it is believed that this is the main reason of rough structures occur.

Because the speckle noise at the defocused plane is determined by the initial random phase chosen in GS algorithm, a multi-exposure method is developed to improve pattern continuity of the single exposure mode. Here, we choose several different initial phases to calculate different CGHs containing the phase information for a desired image and add the intensity of the defocused plane of these CGHs. The optical intensity distribution of these CGHs contains a same desire pattern and different speckle noise. As each CGH is loaded on SLM for a very short time (e.g., 50 ms) in processing, only the overlapped region (desired pattern) by different CGHs can be fully polymerized. Meanwhile, the

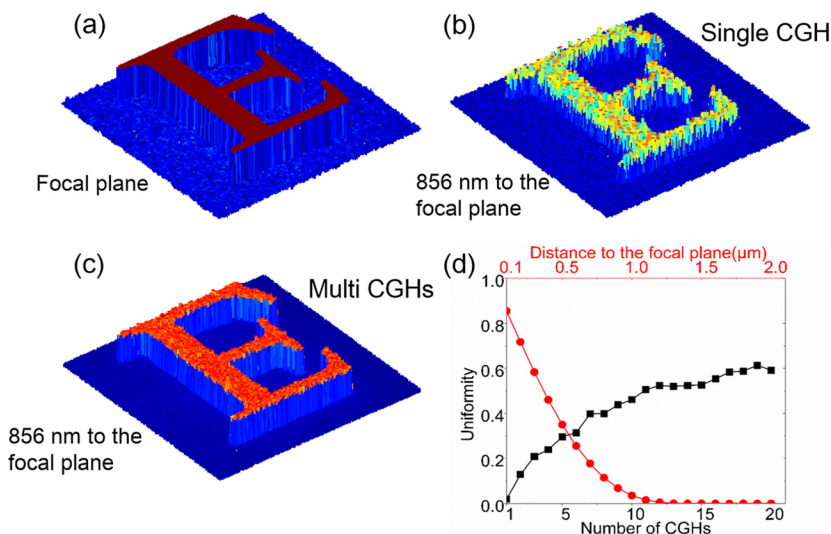


FIG. 2. (a) and (b) are the optical intensity simulations of single-CGH at the focal plane and defocused plane. Obviously, the optical uniformity at the defocused plane is much lower than that at the focal plane. (c) is the optical intensity distribution at the defocused plane of 20 CGHs. (d) is the plot of optical uniformity as a function of number of CGHs (Black square) and defocused position (Red circle).

speckle noise was averaged. Thus, the structure achieved by multi-exposure method is similar to the simulation in Fig. 2(c) in which flawed structures can be greatly improved. We also find that the optical uniformity increases as the number of added CGHs increases, as shown in Fig. 2(d). But, the uniformity decreases as the defocusing amount increases. The optical intensity distribution as a function of number of CGHs is measured at the defocused plane with 865 nm shift to the focal plane. The optical uniformity increases from 0.019 to 0.592 as the number of CGHs increases from 1 to 20. We also found that the uniformity is like an exponential function of defocusing amount. It is 0.856 at 100 nm shift to the focal plane, 0.035 at 900 nm, respectively. It approaches to 0 when the shift amount is bigger than $1.2 \mu\text{m}$.

Shown in Figs. 3(a) and 3(b) are the top-view and magnified scanning electron microscopic (SEM) images of two words “HELLO” and “USTC,” which were achieved by loading a single CGH and 1 second exposure. The fabricated structures are flawed, as compared with that in Fig. 3(c). Each letter in Fig. 3(c) was fabricated by loading 20 preset holograms successively with the irradiation time of 50 ms. The total time for one letter is also 1 s, and the whole words

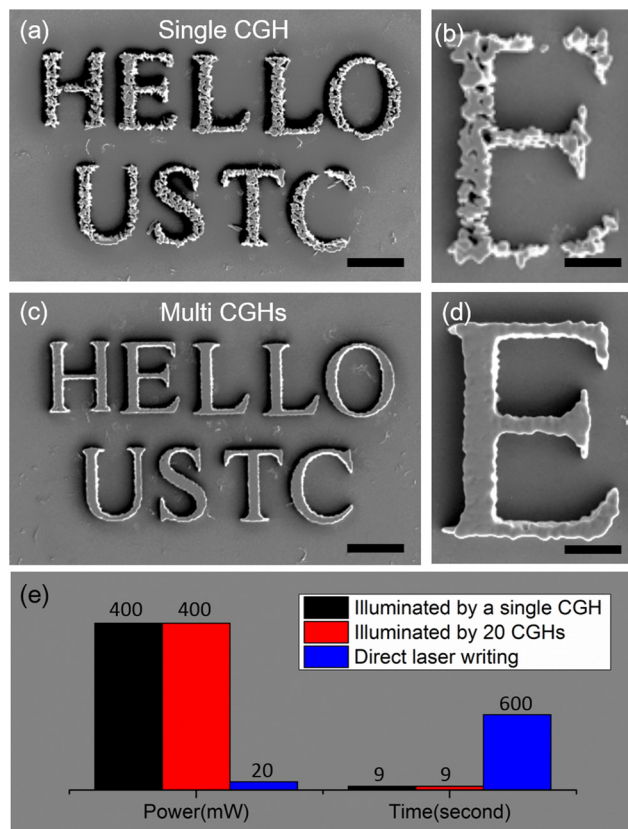


FIG. 3. (a) is the overlooked SEM image of two words “HELLO” and “USTC” achieved by a single exposure of a single CGH for 1 s. (b) is the detail of the flawed letter “E.” (c) is the SEM of the improved result achieved by multi-exposure of 20 CGHs (Every CGH exposure time is 50 ms) loaded on SLM successively. The total time for every letter is also 1 s by multi-CGH exposure, which is the same as that by single-CGH exposure. (d) is the detail of the improved letter “E.” The scale bar is $15 \mu\text{m}$ in (a) and (c), $5 \mu\text{m}$ in (b) and (d). (e) is a comparison of the corresponding laser power and fabrication time for the two words under three kinds of different approaches. The power in multi-CGH exposure is also the same as that by single-CGH exposure (400 mW).

only cost 9 s, while the fabrication time for the two words is bigger than 10 min by direct laser writing (DLW). From the magnified SEM image in Fig. 3(d), we can see that the quality of the letter “E” was obviously improved. The structures by multi-exposure in Fig. 3(d) are much smoother than the ones by single-exposure in Fig. 3(b). Figure 3(e) shows the laser power and fabrication time for the two words under three kinds of different approaches: point-to-point scanning, single-exposure, and multi-exposure. We can find that both of single-exposure and multi-exposure method can reduce the fabrication time from 600 s to 9 s, as compared with point-to-point scanning. But, the quality of the improved multi-exposure method is much better than the one by conventional single-exposure. This will be beneficial for this method to realize more complex microstructures and functional devices for broad practical applications.

As a proof of concept demonstration, this multi-exposure approach was used to rapidly fabricate various Damann gratings or beam splitter. Figures 4(b)–4(d) are the top-view SEM images of different gratings which can generate an array of 2×2 , 5×5 spots. Figures 4(e)–4(g) are the magnified SEM images of various gratings. To get the structures shown in Figs. 4(b) and 4(d), 20 holograms containing the phase information of a pattern were calculated. Each block in the structure is fabricated in 500 ms exposure. Therefore, the whole grating shown in Fig. 4(b) can be achieved in 25 s, and that in Fig. 4(d) needs 32 s. In comparison, they will cost 30 min or more via point-to-point scanning. Parallel fabrication by using multi foci may also decrease the processing time to less than 1 min, but it cannot be applied to fabricate the complex letters in Figure 3 and Damann grating in Figs. 4(c) and 4(f) because the blocks are not the same size or shape. Four series of CGHs carrying the phase information of 4 kinds of blocks were calculated in

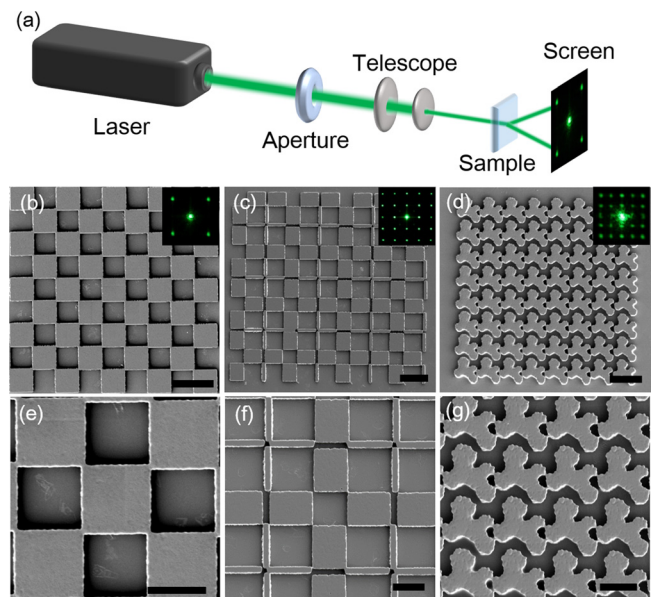


FIG. 4. A home-made optical characterization system was built to investigate their optical properties. (a) Multi-exposure fabrication of various Damann gratings which can generate 2×2 (b) and 5×5 (c) spots array. (d) is a complex beam splitter which can generate 5×5 spots array. The top right corners are the diffraction patterns of gratings. (e)–(g) are the details of (b)–(d). Scale bars are $20 \mu\text{m}$ in (b)–(d) and $10 \mu\text{m}$ in (e)–(g).

advance. The smaller blocks cost 500 ms, while the bigger ones need 1 s. Thus, the Dammann grating with $200\ \mu\text{m} \times 200\ \mu\text{m}$ area [Fig. 4(c)] can be achieved in 90 s. To investigate their optical properties, a home-made optical characterization system was built, as shown in Fig. 4(a). A He:Ne laser with 532 nm wavelength is used to generate the incident light, and a CCD is used to capture the focused diffractive pattern. Experimentally, an array of 2×2 , 5×5 spots [The insets of Figs. 4(b)–4(d)] were obtained, just as what we expected.

For binary optical devices, the thickness of photoresist is $\Delta nd = \varphi/k$, an important parameter for the diffractive efficiency. Here, Δn is the difference between the indexes of photoresist and air, d is the thickness of photoresist, and φ is the phase shift of the incident light and k is the wavenumber, respectively. To get the optimal diffractive efficiency, φ should be odd times of π . As the Dammann grating is designed for 532 nm wavelength and the index of SZ2080 is 1.5 for 532 nm wavelength and that of air is 1, the thickness of photoresist should be odd times of 532 nm. To make sure that the thickness is exactly equal to the theoretical value, the parameter in spin-coating process must be carefully chosen. In detail, the photoresist is mixed with acetone with the volume ratio of 2:1. By 4000 rpm-speed spin coating for 45 s, the thickness of photoresist is about $1.6\ \mu\text{m}$, which is about 3 times of the wavelength of the incident light. So, the phase change of the laser through the sample is about π . The diffractive efficiency (η) is $\eta_{\text{odd}} = (I_0 + 2 \sum_{i=1}^N I_i)/I_{\text{inc}}$ for an odd-number-spot generator. Here, I_0 is the intensity of zero order light, and I_i is that of higher order, respectively. I_{inc} is the intensity of the incident light. The diffractive efficiency of the grating showed in Fig. 4(c) is 37%.

In conclusion, we have proposed a multi-exposure technique using tens of CGHs successively loaded on SLM to effectively improve the non-uniformity of optical field intensity at the defocused plane from ~ 0.02 to ~ 0.6 and eliminate the speckle noise. For comparison, two series of letters “HELLO” and “USTC” were fabricated through a single exposure and multi exposure, which further confirmed that the multi-exposure approach can greatly improve the surface quality without losing efficiency. Finally, we also demonstrated that this method has excellent flexibility to rapidly

fabricate several kinds of complex beam splitters with high quality, such as 2×2 , 5×5 Daman and complex nonseparate 5×5 gratings. We believed that the multi-exposure SLM-TPP method will find broader applications in fabricating various microoptical, microfluidics, micromechanical devices, and biological scaffold microstructures.

This work was supported by National Natural Science Foundation of China (Nos. 51275502, 61475149, 51405464, 91223203), Anhui Provincial Natural Science Foundation (No. 1408085ME104), National Basic Research Program of China (No. 2011CB302100), and the Fundamental Research Funds for the Central Universities (WK2090090012).

- ¹H. Lin, B. Jia, and M. Gu, *Opt. Lett.* **36**, 406 (2011).
- ²S. Zhang, Y. Li, Z. Liu, J. Ren, Y. Xiao, H. Yang, and Q. Gong, *Appl. Phys. Lett.* **105**, 061101 (2014).
- ³W. Xiong, Y. S. Zhou, X. N. He, Y. Gao, M. Mahjouri-Samani, L. Jiang, T. Baldacchini, and Y. F. Lu, *Light: Sci. Appl.* **1**(4), e6 (2012).
- ⁴H. Sun and S. Kawata, *J. Lightwave Technol.* **21**(3), 624 (2003).
- ⁵S. Matsuo, S. Juodkazis, and H. Misawa, *Appl. Phys. A* **80**, 683 (2005).
- ⁶Y. Hayasaki, T. Sugimoto, A. Takita, and N. Nishida, *Appl. Phys. Lett.* **87**, 031101 (2005).
- ⁷T. Kondo, S. Matsuo, S. Juodkazis, and H. Misawa, *Appl. Phys. Lett.* **79**, 725 (2001).
- ⁸H. Takahashi, S. Hasegawa, A. Takita, and Y. Hayasaki, *Opt. Express* **16**, 16592 (2008).
- ⁹Y. Hu, Y. Chen, J. Ma, J. Li, W. Huang, and J. Chu, *Appl. Phys. Lett.* **103**, 141112 (2013).
- ¹⁰Y. Tian, Y. Zhang, J. Ku, Y. He, B. Xu, Q. Chen, H. Xia, and H. Sun, *Lab Chip* **10**, 2902 (2010).
- ¹¹S. D. Gittard, A. Nguyen, K. Obata, A. Koroleva, R. J. Narayan, and B. N. Chichkov, *Biomed. Opt. Express* **2**, 3167 (2011).
- ¹²M. Sakakura, T. Sawano, Y. Shimotsuma, K. Miura, and K. Hirao, *Opt. Express* **18**, 12136 (2010).
- ¹³L. Yang, A. El-Tamer, U. Hinze, J. Li, Y. Hu, W. Huang, J. Chu, and B. N. Chichkov, *Appl. Phys. Lett.* **105**, 41110 (2014).
- ¹⁴C. Hnatovsky, V. G. Shvedov, W. Krolikowski, and A. V. Rode, *Opt. Lett.* **35**, 3417 (2010).
- ¹⁵C. Zhang, Y. Hu, J. Li, G. Li, J. Chu, and W. Huang, *Opt. Express* **22**, 3983 (2014).
- ¹⁶M. Duocastella and C. B. Arnold, *Laser Photonics Rev.* **6**, 607 (2012).
- ¹⁷B. Mills, J. A. Grant-Jacob, M. Feinaeugle, and R. W. Eason, *Opt. Express* **21**, 14853 (2013).
- ¹⁸J. Amako, H. Miura, and T. Sonehara, *Appl. Opt.* **34**, 3165 (1995).
- ¹⁹L. Yang, J. Li, Y. Hu, C. Zhang, Z. Lao, W. Huang, and J. Chu, *Opt. Commun.* **331**, 82 (2014).
- ²⁰R. Di Leonardo, F. Ianni, and G. Ruocco, *Opt. Express* **15**, 1913 (2007).